AD_____

Award Number: DAMD17-96-1-6139

TITLE: X-Photon-to-Information Conversion Efficiency in Digital Telemammography

PRINCIPAL INVESTIGATOR: Celeste B. Williams
Bradley D. Clymer, Ph.D.

CONTRACTING ORGANIZATION: The Ohio State University Research Foundation
Columbus, Ohio 43210-1063

REPORT DATE: June 1999

TYPE OF REPORT: Annual

PREPARED FOR: U.S. Army Medical Research and Materiel Command
Fort Detrick, Maryland 21702-5012

REPORT DOCUMENTATION PAGE

Form Approved
OMB No. 074-0188

1. AGENCY USE ONLY (Leave blank)	2. REPORT DATE	3. REPORT TYPE AND DATES COVERED
	June 1999	Annual (1 Jun 98 - 31 May 99)

4. TITLE AND SUBTITLE
X-Photon-to-Information Conversion Efficiency in Digital Telemammography

5. FUNDING NUMBERS
DAMD17-96-1-6139

6. AUTHOR(S)
Celeste B. Williams
Bradley D. Clymer, Ph.D.

7. PERFORMING ORGANIZATION NAME(S) AND ADDRESS(ES)
The Ohio State University Research Foundation
Columbus, Ohio 43210-1063

E-Mail: CLYMER.1@OSU.EDU

8. PERFORMING ORGANIZATION REPORT NUMBER

9. SPONSORING / MONITORING AGENCY NAME(S) AND ADDRESS(ES)
U.S. Army Medical Research and Materiel Command
Fort Detrick, Maryland 21702-5012

10. SPONSORING / MONITORING AGENCY REPORT NUMBER

11. SUPPLEMENTARY NOTES

12a. DISTRIBUTION / AVAILABILITY STATEMENT
Approved for Public Release; Distribution Unlimited

12b. DISTRIBUTION CODE

13. ABSTRACT ***(Maximum 200 Words)***

Imaging techniques for diagnosis and detection of breast cancer deform the breast from its original shape by applying external forces. However, these methods do not take into account the mechanical nature of breast tissue. It is known that pathology has different elastic properties than healthy tissue and the characterization of the mechanical nature of tissue may act as a diagnostic tool, which may improve the prognosis for breast cancer patients. This research is based on these factors of breast cancer research. The purpose of this study is to non-invasively estimate the *in vivo* force-deformation behavior of normal breast tissue undergoing mild compression.

14. SUBJECT TERMS
Breast Cancer

15. NUMBER OF PAGES
31

16. PRICE CODE

17. SECURITY CLASSIFICATION OF REPORT	18. SECURITY CLASSIFICATION OF THIS PAGE	19. SECURITY CLASSIFICATION OF ABSTRACT	20. LIMITATION OF ABSTRACT
Unclassified	Unclassified	Unclassified	Unlimited

FOREWORD

Opinions, interpretations, conclusions and recommendations are those of the author and are not necessarily endorsed by the U.S. Army.

_____ Where copyrighted material is quoted, permission has been obtained to use such material.

_____ Where material from documents designated for limited distribution is quoted, permission has been obtained to use the material.

_____ Citations of commercial organizations and trade names in this report do not constitute an official Department of Army endorsement or approval of the products or services of these organizations.

_____ In conducting research using animals, the investigator(s) adhered to the "Guide for the Care and Use of Laboratory Animals," prepared by the Committee on Care and use of Laboratory Animals of the Institute of Laboratory Resources, national Research Council (NIH Publication No. 86-23, Revised 1985).

_____ For the protection of human subjects, the investigator(s) adhered to policies of applicable Federal Law 45 CFR 46.

_____ In conducting research utilizing recombinant DNA technology, the investigator(s) adhered to current guidelines promulgated by the National Institutes of Health.

_____ In the conduct of research utilizing recombinant DNA, the investigator(s) adhered to the NIH Guidelines for Research Involving Recombinant DNA Molecules.

_____ In the conduct of research involving hazardous organisms, the investigator(s) adhered to the CDC-NIH Guide for Biosafety in Microbiological and Biomedical Laboratories.

Celeste Ott 6/28/99

PI - Signature Date

Table of Contents

INTRODUCTION

This project is based on two factors in breast cancer research. First, pathology has different elastic properties than healthy tissue, and second, conventional methods for diagnosis and detection of breast cancer are all performed by deforming the breast. An understanding of the biomechanical properties of breast tissue may aid the development of accurate breast models, and the characterization of the mechanical nature of tissue may provide diagnostic information.

This report describes present research and tasks completed according to the BAA proposal. In keeping with the goals outlined in the Statement of Work, the main objectives of the third year of research were to:

- Focus on incremental compression to obtain small deformations
- Estimate the *in vivo* stress from the deformation data
- Measure the normal stress
- Implement 2D algorithms with tissue biomechanical properties

BODY OF REPORT

BACKGROUND

Mechanical Deformation

The biomechanical nature of soft tissue is described in terms of its stress - strain or constitutive relationship. The particular shape of the deformation is a function of both the internal strains and stresses within the tissue, and the external forces applied to the tissue. A constitutive model for a material can be described using the strain energy density function, (SEDF). Fung, [see reference 1], first introduced modeling of the stress-strain relationship using the SEDF to soft tissue mechanics in 1967. Several forms of the SEDF have been proposed for different types of materials. One form of the SEDF is a polynomial relationship where

$$U = \sum_{i+j=1}^{N} C_{ij} (I_1 - 3)^i (I_2 - 3)^j$$

N is defined as the complexity of the polynomial. C_{01} and C_{10} are constants, and I_1, I_2 are strain invariants. The simplest form of the polynomial SEDF is the Moony-Rivlin model, which for volume incompressible materials has the form

$$U = C_{10}(I_1 - 3) + C_{01}(I_2 - 3)$$

Deformable models

A major constraint in modeling of soft tissue is that the model should correctly represent the deformability of real tissue undergoing pressures similar to those occurring in real-life applications. Image morphing is useful in displaying deformation because the displacements can be smooth from one position to another. Two-dimensional morphing techniques, such as free form deformation (FFD) and feature-based morphing are abundant and widely used in image morphing. However, morphing algorithms can only accurately simulate small deformations.

For large deformations, foldover can occur. Foldover is defined as the overlapping of control points that induces distortions and undesirable wrinkles into the resulting images. In addition, while existing 2D morphing algorithms efficiently simulate small deformation, they ignore physical principles of deformation and therefore are difficult to incorporate into real-life and real-time applications. One way of overcoming the limitations of morphing algorithms is through the use of finite element models.

Finite Element Modeling

Finite element models are capable of simulating a wide variety of materials, loading, and boundary conditions. With FEM, real-situation loading can be applied to the model, and the model can also be designed using experimental deformation data. FEM describes a volume or surface as a set of basic elements. The volume of an object is divided into subregions of finite elements, and each element possesses the material properties of the object, (e.g., steel, rubber, soft tissue). Associated with each element are nodes at which adjacent elements are linked together. Typical finite elements are shown in Figure 1. Finite element analysis involves estimating a continuous function by approximating the values at finite number of points within the domain. The accuracy of the solution increases with number of points (i.e., nodes) used.

METHODS

In the next sections, the term compression is used in the mammographic sense in which the thickness of the breast is reduced by parallel plates. A coil-compression device was designed to fulfill the need of uniaxially deforming the breast tissue *in vivo*. With the apparatus, the mechanical behavior of normal breast tissue at small (static) compressive strains can be observed. Using the device, shown in Figure 2, we performed medial-lateral compressions of a single breast and imaged the entire breast. Deformation data were obtained *in vivo* using magnetic resonance imaging to detect regions of interest, (i.e., landmarks). Imaging was performed on a GE 1.5 T clinical MR system (General Electric, Signa, Milwaukee, WI) using a 3D-FSPGR (fast spoiled gradient echo) sequence, with TE= 4.2 msec, TR=25 msec, flip angle = 60 degrees, and a resolution of 0.4 mm x 0.4mm x 0.7 mm.

Imaging was performed on several subjects (N=4). Test subjects were healthy female volunteers, over the age of 18 and pre-menopausal. Incremental compressions were obtained by varying the width between the top and bottom plates using mechanical spacers and stops. With small incremental deformations (<10%), corresponding landmarks could be easily mapped between deformed (compressed) and undeformed (uncompressed) images.

To address the problem of image registration and localization of landmarks, external markers were placed on the breast in a circular pattern. The markers consisted of small drops of a metallic polish that introduced susceptibly artifacts into the MR images (see Figure 3). With the markers, rigid motion transformations (i.e., translation and rotation) were easily determined. Separate external gel-filled markers were employed to provide a means of correcting the signal intensity drop-off commonly observed when imaging with a rf surface coil [2].

To measure the normal stress at specific landmarks, flexible Uniforce© force sensors (Force Imaging Technologies, Chicago, IL) were arranged in a linear pattern and placed beneath the top plate such that the sensing area of each sensor was in contact with the surface of the breast. The flexible sensors, shown in Figure 4, are thin (about 0.076 mm) and the sensing area has a diameter = 0.25 in. Before imaging, sensors were calibrated and preconditioned to obtain the typical calibration curve shown in Figure 4b.

In order to develop a finite element representation of the deformation of breast tissue, the ABAQUS [see reference 3] finite element software package was employed to describe the behavior of breast tissue using experimental data. ABAQUS is capable of handling complex materials properties such as non-linearity, volume compressibility and viscoelasticity, as well as complex loading such as static, quasi-static, and dynamic compression.

RESULTS AND DISCUSSION

Preliminary Studies

Axial and Transverse Strain

To obtain deformation data, the top plate is moved to a position to achieve an overall breast compression that is <20%. The normal forces measured by each sensor are recorded and next the subject is placed inside the magnet bore and imaged for 7 minutes. Coronal images of the breast are obtained and displacement is localized on the corresponding MR images (that is, uncompressed and compressed images) using internal and external landmarks. Strain is calculated using the lengths of line segments between paired points, (see Figure 5). The paired points are the regions where each sensor in the array is located. Line segments are used because of their invariant properties. The displacement of the segment, in length or angle, in the direction of the applied compressive load is used to determine the axial strain, (ε_y). Transverse strain, (ε_x), is the strain that is perpendicular to the direction of the applied force. Lateral line segments are used to calculate transverse strain. The axial and transverse strains are defined as

$$\varepsilon_y = \frac{\Delta y}{y_o} \quad \text{and} \quad \varepsilon_x = \frac{\Delta x}{x_o}$$

where y_o is the y-component of the line segment in the undeformed volume, $\Delta y = y - y_o$, and y is the y-component of the corresponding line segment in the deformed volume. In the transverse strain, x_o is the x-component of the line segment in the undeformed volume, $\Delta x = x - x_o$, and x is the x-component of the line segment in the deformed volume. Table 1 indicates the axial and transverse strains calculated for two compressions, low (<20 %) and high (>20%), performed on subjects 1 and 2. From the strain bar graphs shown in Figures 6 and 7, the axial strain is observed to increase as breast compression is increased from 9% to 27%. However, the transverse strain decreases as breast compression varies from 9% to 27%. This decrease in transverse strain is due to the fact that the pectoral muscle limits transverse displacement.

In order to obtain 3D displacement data, the tissue is segmented and volume rendered to obtain a 3D visualization of the breast tissue, (see Figure 8). The displacement in three directions is evaluated using the displacement vector. The displacement vector, **D**, is defined as the displacement of a point P (x, y, z) in the undeformed volume, to the point P′(x′, y′, z′) in the deformed volume. It has the form

$$\mathbf{D} = u\hat{\mathbf{x}} + v\hat{\mathbf{y}} + w\hat{\mathbf{z}}$$

where the vector components are $u = x' - x$, $v = y' - y$, and $w = z' - z$ .The graphs of the vector components, shown in Figures 9a-c, represent the displacement of four corresponding internal landmarks. The graphs indicate that as compressive loading increases, the y-displacement contracts or compresses more (i.e., the negative sign indicates contracting movement). The x-displacement is observed to decrease as the applied loading increases. This is similar to what occurs in the transverse strain. The z-displacement (out-of-plane deformation) is more complex. This displacement clearly cannot be neglected as some earlier works into tissue mechanics once assumed [1,4].

Load-Strain Relationship

The normal stress-normal strain relationship is obtained by fitting the stress and strain data using a non-linear least squares technique and plotting the normal stress against the axial (or normal) strain. Normal stress, σ_y, is calculated using the equation

$$\sigma_y = \text{force/area} \quad (N/m^2)$$

where the area is the cross-sectional area of the breast in contact with the force sensor. For the external compressive forces exerted on the breast by the compression device, sensors with a range of 0 to 2.2 N are appropriate for measuring force. The stress-strain plots, (shown in Figure 10), were obtained for two different subjects 3 and 4. Subject 3 has denser breast tissue than Subject 4. The stress-strain curves exhibit the typical characteristics of soft tissue.

Finite Element Analysis

The finite element model is derived using the MR measurements of strain. The model is intended to reflect the large deformation of breast tissue undergoing static compressive loading. Materials that undergo large elastic deformations are usually characterized as hyperelastic, and under static loading conditions, soft tissues can be viewed as hyperelastic. Such a method has been used to model brain tissue under large deformations [5]. The breast is modeled using two approaches: one with the tissue standing alone, and the other with the skin and the tissue. The skin is modeled with membrane elements and elastic material parameters of Young's modulus = 3×10^6 Pa and Poisson's ratio (volume compressibility) = 4.3. Membrane elements are used to represent thin surfaces in space. Such elements offer strength in the plane of the element but have no bending stiffness, (e.g., the thin rubber sheet that forms a balloon). The membrane element mesh, shown in Figure 11, is modeled with 75 eight-node elements and 226 nodes.

A simple mesh, shown in Figure 12, can be generated with the tissue attached to the skin at the areola, (i.e., the front of the mesh). A body force is applied to the left side of the mesh, where the breast rests on the bottom plate, and a distributed force representing the normal force is applied to the right side of the mesh. The right side of the mesh represents where the top plate is fastened down to supply an uniaxial compressive loading. Friction and slip are neglected at the surfaces of the top and bottom plates because fudicial markers indicate that this movement is negligible. However, to more accurately simulate mammography loading, finite slip may be added to the model in the future. To simulate non-slip boundaries, the nodes on the right and left sides of the mesh are constrained in the x and y directions of the global coordinate system (shown as 3 and 1, respectively, in Figure 12). The back nodes of the membrane or skin mesh are constrained in the x, y, and z directions to simulate the attachment of the skin to the chest wall. The breast tissue model is developed using 300 twenty-node quadrilateral continuum elements, (see Figure 1). Solid or continuum elements are used for complex nonlinear stress analysis involving large deformations. The tissue is modeled as a hyperelastic material using the Mooney-Rivlin form of the SEDF. With the ABAQUS finite element package, the constitutive model parameters can be estimated from test data to obtain material parameters. In order to obtain the C_{ij} coefficients, the experimental normal stress-strain data are used. The coefficients can also be estimated from the equation

$$\sigma_R = C_{10} + C_{01}/\lambda_1$$

where σ_R is the reduced stress and λ_1 is the stretch ratio, (i.e., λ_1 = deformed length/ undeformed length). A plot of σ_R versus $1/\lambda_1$ has a slope equal to C_{01} and an intercept equal to C_{10}. The plot of σ_R versus $1/\lambda_1$ is shown in Figure 13, and the slope and intercept are 12.24 kPa and 13.23 kPa, respectively.

Significance

All objectives of the proposed research are on track and proceeding as scheduled. Task 4 has been completed and Task 5 has been initiated.

TASK 4: Investigate morphing algorithms, Finite element methods and thin plate splines, FFD, and volume morphing.

TASK 5: Acquire deformation data. Estimate stress. Develop constitutive relationship.

The results of this work were presented on May 27,1999 at ISMRM [6] (see appendix b).

In keeping with the goals outlined in the Statement of Work, our next research steps are to:

- Model the mesh for representation of branching tissue and implement out-of-plane deformation

- Develop Constitutive relationship

We are developing manuscripts for journal papers to document the work on measuring *in vivo* stresses and strains for submission during the next six months.

CONCLUSIONS

From the deformation studies, we found that MR imaging can provide quantitative *in vivo* biomechanical information about breast tissue subjected to incremental compressions. From the force sensors, measurements of the normal stress during static compression were obtained and the stress-strain curves evaluated were typical for soft tissue. With the estimates of *in vivo* strain and stress, incorporating the strain energy density function (SEDF) into finite element modeling approximated a constitutive model of breast tissue under mild compressive deformation.

With the ABAQUS package, complex modeling can be achieved, however the software is limited in generating more complex geometrical mesh shapes that are required for displaying the out-of-plane branching of breast tissue. Figure 14 shows an example of a complex geometrical mesh of breast tissue. A new mesh generation software that can be incorporated into ABAQUS is currently under investigation.

While computer morphing has proven beneficial in 2D morphing, it has proven problematic in 3D morphing. As can be observed from the 3D volumes, it is difficult to identify enough point and line features to control a morphing process. Hence after the initial morphing was investigated, it was decided to concentrate more on developing a deformable finite element model.

REFERENCES

1. Fung. Y.C., Biomechanics: Mechanical Properties of Living Tissues. Springer-Verlag, New York, 1993.

2. Chakeres, D., Schmalbrock, P., Clymer, B., Deak, G., ***Williams, C.***, "MR Surface Coil Image Correction Using an Integrated Positional Reference System", submitted to Radiological Society of North America, 84th Scientific Assembly and Annual Meeting, 1998.

3. ABAQUS, Version 5.7, Hibbit, Karlsson and Sorensen, Providence, RI., 1997.

4. Gallagher, R., Simon, B., Johnson, P., Gross, J., Finite Elements in Biomechanics, Wiley & Sons, New York, 1982.

5. Mendis, K., Stalnaker, R., Advani, S., "A constitutive relationship for large deformation finite element modeling of brain tissue", Journal of Biomechanical Engineering, Vol. 117, pp. 279-285, August 1995.

6. ***Williams, C.***, Clymer, B., Schmalbrock, P., "Biomechanics of Breast Tissue: Preliminary studies into force-deformation relationship", submitted to International Society For Magnetic Resonance in Medicine, 70th Scientific Meeting and Exhibition, 1999.

APPENDICES

a. Acronyms and Symbols

T - tesla

TR - repetition time

TE - echo time

T1- spin-lattice relaxation time of the magnetization along the longitudinal axis

T2- spin-spin relaxation time of magnetization in the transverse plane.

msec - millisecond

mm - millimeter

SNR - signal-to-noise ratio

SPGR- spoiled gradient echo

2D - two dimensional

3D - three dimensional

C-C - cranio-caudal

M-L - medio-lateral

A-P – anterior-posterior

Deformation - $Z_o - Z / Z_o$

N - Newton

Pa = Pascal (N/m^2)

b. Abstracts

Biomechanics of Breast Tissue: Preliminary study of force -deformation relationship

Celeste. Williams [(1)], Bradley. Clymer, PhD [(2)], Petra Schmalbrock, PhD [(3)]
The Ohio State University, Columbus, Ohio
(1) Biomedical Engineering Center, (2) Dept. of Electrical Engineering, (3) Dept. of Radiology,

INTRODUCTION

Conventional imaging techniques for diagnosis and detection of breast cancer deform the breast by applying external forces. The mechanical nature of breast tissue is not taken into account because the biomechanical behavior of soft tissue is not fully understood [1]. Pathology has different elastic properties from healthy tissue and the characterization of the mechanical nature of tissue may serve as a diagnostic tool, which may improve the prognosis for breast cancer patients. The purpose of this study is to noninvasively estimate the *in vivo* force-deformation behavior of normal breast tissue undergoing mild compression.

Deformation Mechanics

The breast is a composite of mechanically different materials. It is composed of several tissue types: glandular, fibrous and adipose (fat). The mammary gland is composed of 5-10 separate branching glands. The structural arrangements consist of 12-18 lobe systems branching from the nipple. The ductal system comprises about 10-15% of the total breast mass. The remaining 85% is mostly adipose tissue [2]. Both adipose and glandular tissues obtain their elasticity from elastic fibers. The mechanical nature of soft tissue is described in terms of its stress-strain relationship.

METHODS

Tissue deformation studies were conducted *in vivo,* with the breast under mild uniaxial compression, using a specially designed coil-compression device. MRI (3D-SPGR) was used to detect displacement of regions of interest (i.e., landmarks). Imaging was done with each subject lying on her side with the right breast compressed in the medial-lateral direction (see figure 1). In this configuration, displacement and normal stress were experimentally evaluated.

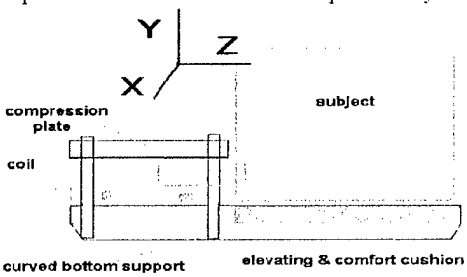

FIGURE 1. Compression configuration.

Stress Sensors

An array of Uniforce© sensors was used to measure normal stress (i.e., force/area) at landmarks. The thin, flexible sensor is constructed of two layers of a nonconductive resistive substrate, which allows the sensor to be adhered to the skin without inducing harmful heating or susceptibilities. The array was placed between the compression plate and the breast, and sensors were capable of detecting static forces over a range of 0 – 4.4N. Force was determined by measuring the change in resistance. The sensor output, in units of newtons, was digitized and displayed on a computer.

RESULTS AND DISCUSSION

Displacement and Deformation

Subjects were imaged with a range of compressions. The widths and percent of deformation of the breast are given in Table 1.

TABLE 1. Percent compression in the direction of the applied force.

uncompressed width (mm)	**100**	**77**	**55**	**75**
compressed width (mm)	**80**	**57**	**35**	**55**
% compression in Y direction	**20.0**	**26.0**	**36.4**	**26.7**

In mechanics, the displacement vector (**D**) represents the displacement of a point (P) located at (x, y, z) in the original volume, to a displaced point (P') located at (x', y', z') in the deformed volume. The displacement vector is

$$\mathbf{D} = u\,\mathbf{x} + v\,\mathbf{y} + w\,\mathbf{z}$$

where the vector components are $u = x' - x$, $v = y' - y$, $w = z' - z$.

Strain is evaluated from the vector components. Figure 2 shows the vector components of specific regions of interest in breast tissue as the whole breast is compressed from 5 to 15 %.

FIGURE 2. Components of displacement vector for landmarks.

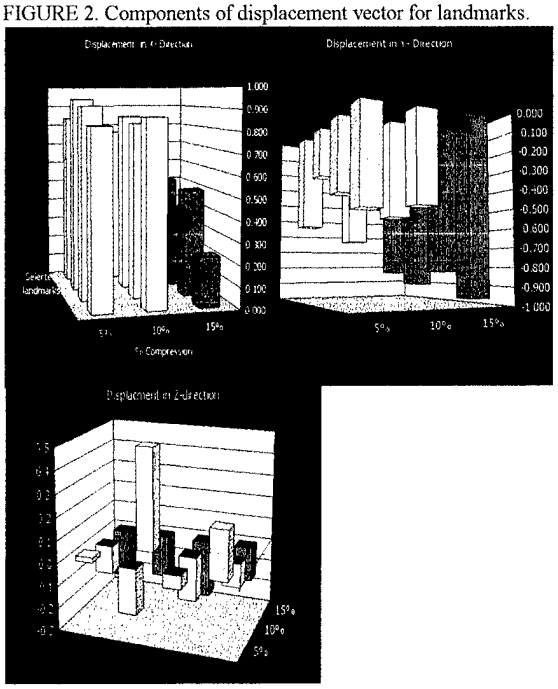

In the graphs, the Y-axis is the Medial-Lateral direction (direction of applied force), the X-axis is in the Cranial-Caudal direction, and Z-axis is from the nipple to chest wall.

Force Measurements

For the *in vivo* stress studies, the sensor array was placed on the top plate in contact with the breast about 1.5 inches from the nipple with sensor connectors at least 2 cm away from the breast to minimize artifacts. The sensors were calibrated and conditioned before and after imaging and the calibration curves show that $\mathbf{B}_0$ does not effect the accuracy of the sensors. Stress data (i.e. force per area) is reported in Table 2.

TABLE 2. Normal stress data from three sensors

SENSOR #	FORCE (N)	STRESS (N/m^2)
1	58.8×10^{-3}	364.5
2	9.81×10^{-3}	60.8
3	88.3×10^{-3}	547.4

REFERENCES

1. Fung. Y.C., Biomechanics: Mechanical Properties of Living Tissues. Springer-Verlag, New York, 1993.

2. Gallagher, R., Simon, B., Johnson, P., Gross, J., Finite Elements in Biomechanics, Wiley & Sons, New York, 1982.

c. Figures

FIGURES 1-14

TABLE 1. Axial strains (ε_y) and transverse strains (ε_x)

AXIAL STRAIN	Subject 1		Subject 2	
	9% compression	27% compression	15% compression	30% compression
	15.91	16.22	12.5	28.57
	15.38	27.27	16.29	10.21
	—	37.50		
	6.25	20.00	4.87	14.92
	-12.50	22.22		
	2.38	21.95		
	—	14.29		
	-11.11	10.00		
	-24.01	24.40		
TRANVERSE STAIN				
	12.84	-5.26	0.07	-14.28
	-74.31	19.75	-4.16	-5.76
	-18.87	9.66		
	16.44	-6.57		

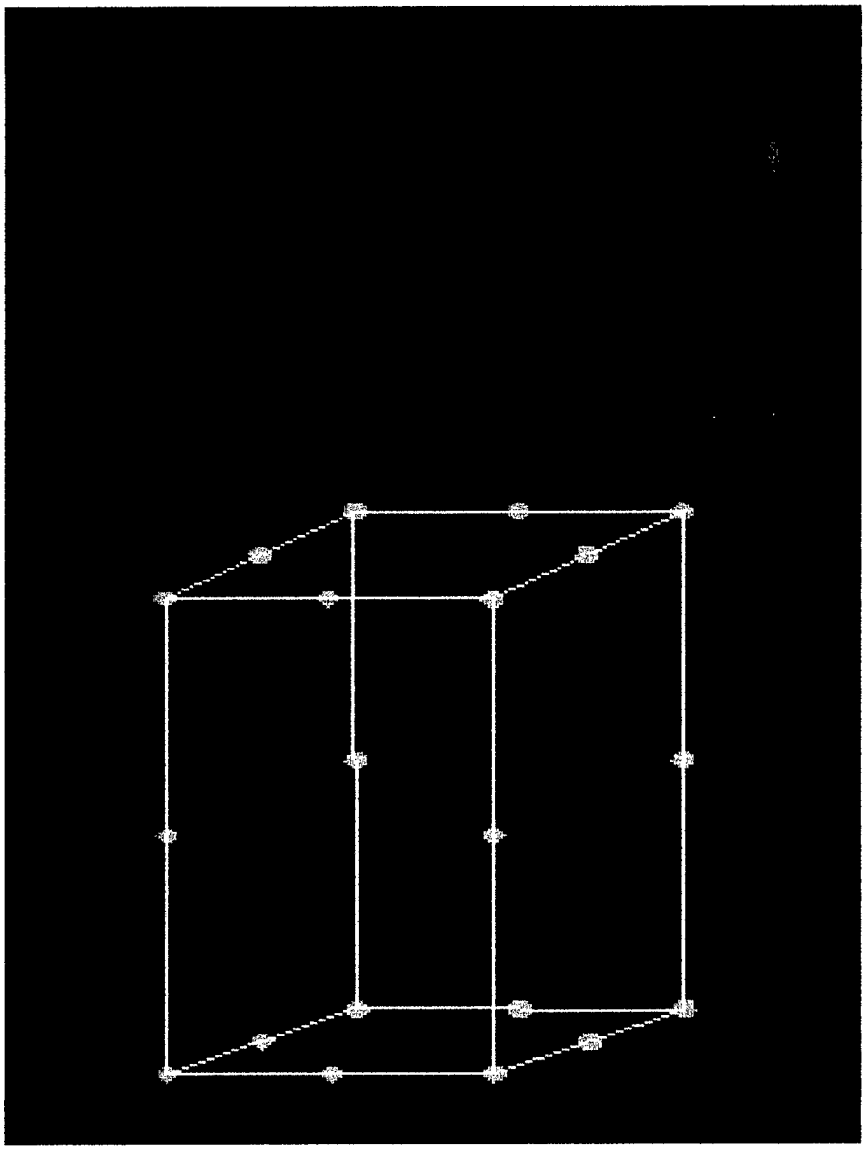

FIGURE 1. Elements used in FE modeling.

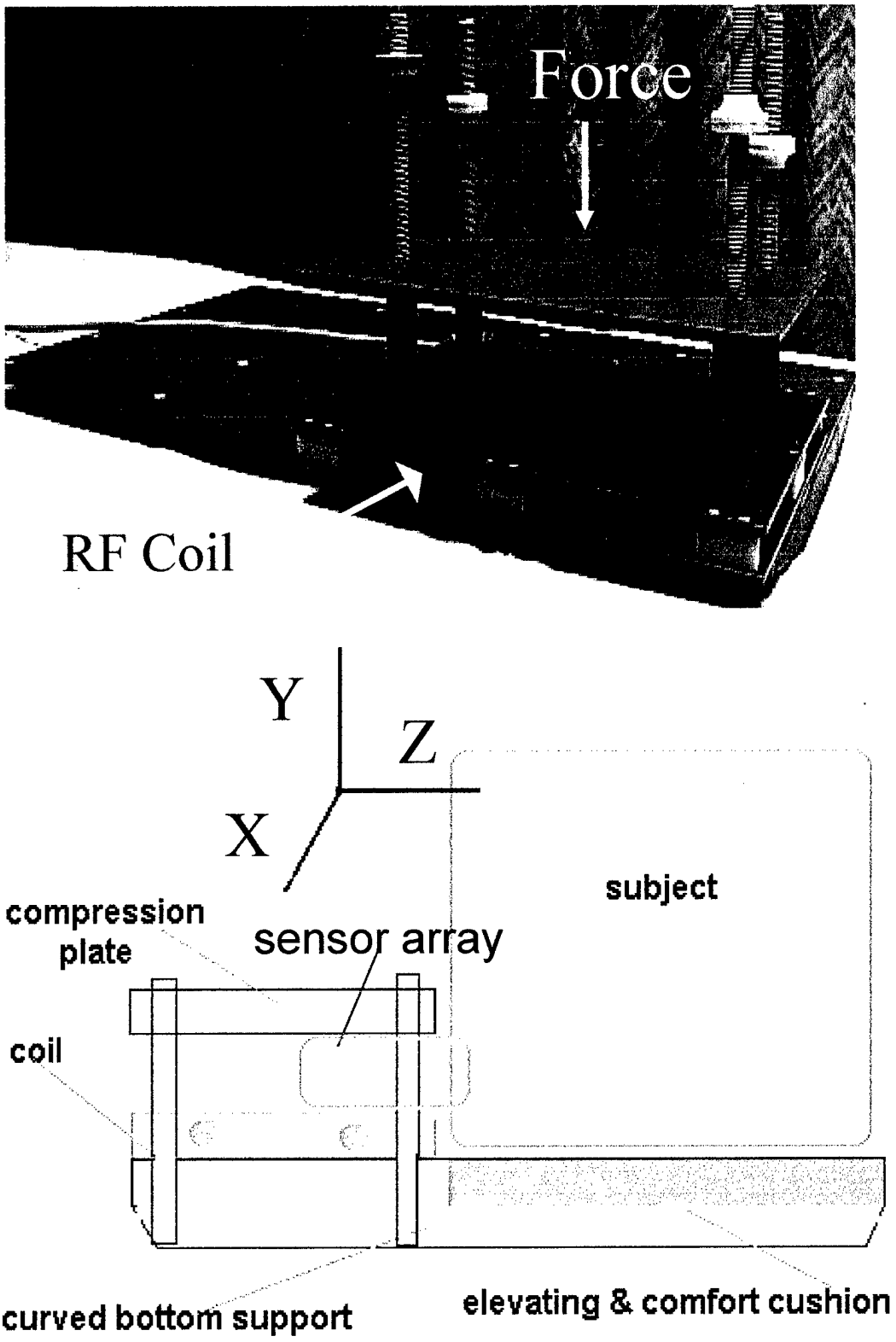

FIGURE 2 (a) Photo of coil-compression device.
(b) Schematic of device

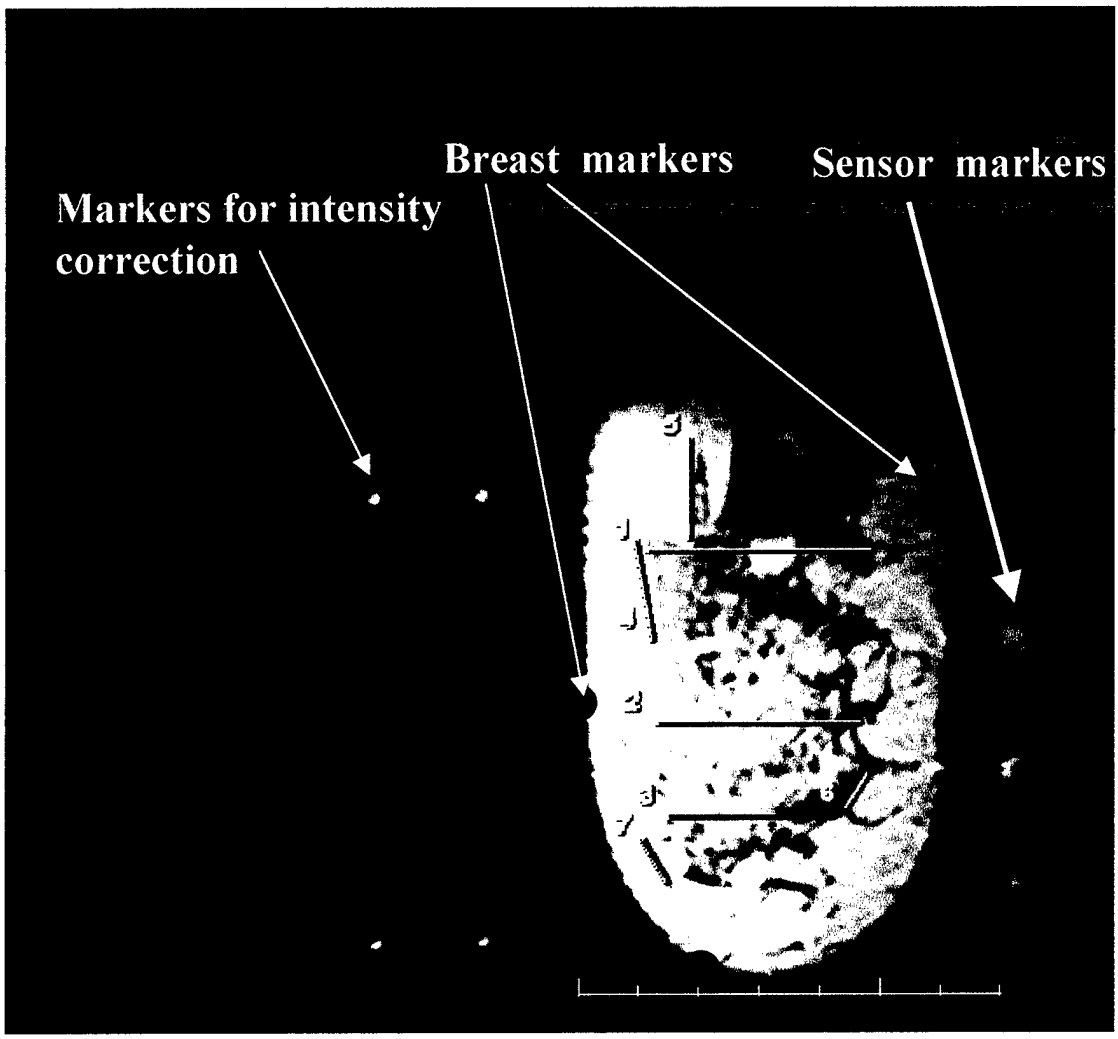

FIGURE 3. Diagram of external markers

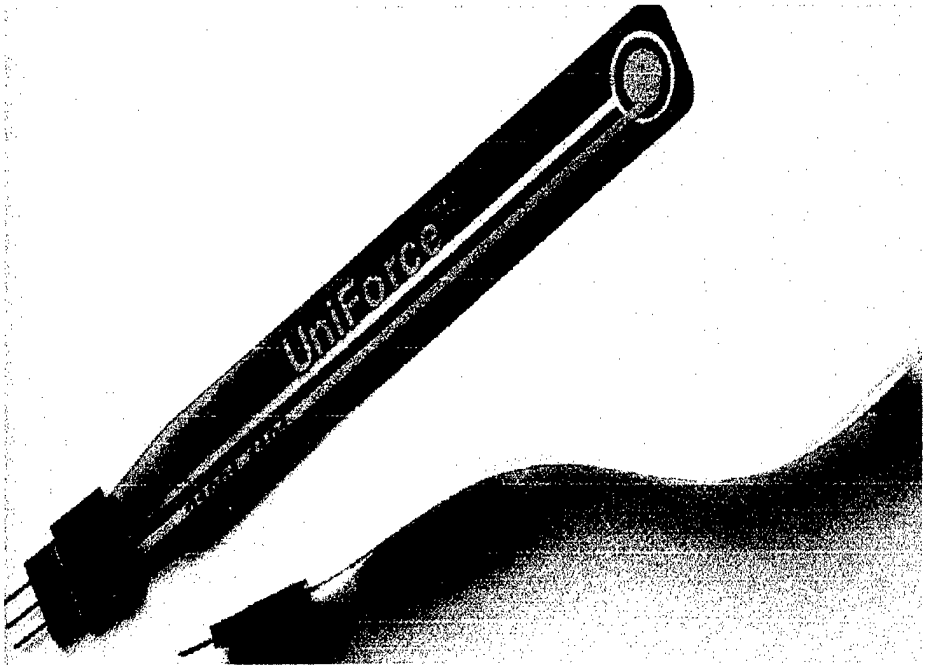

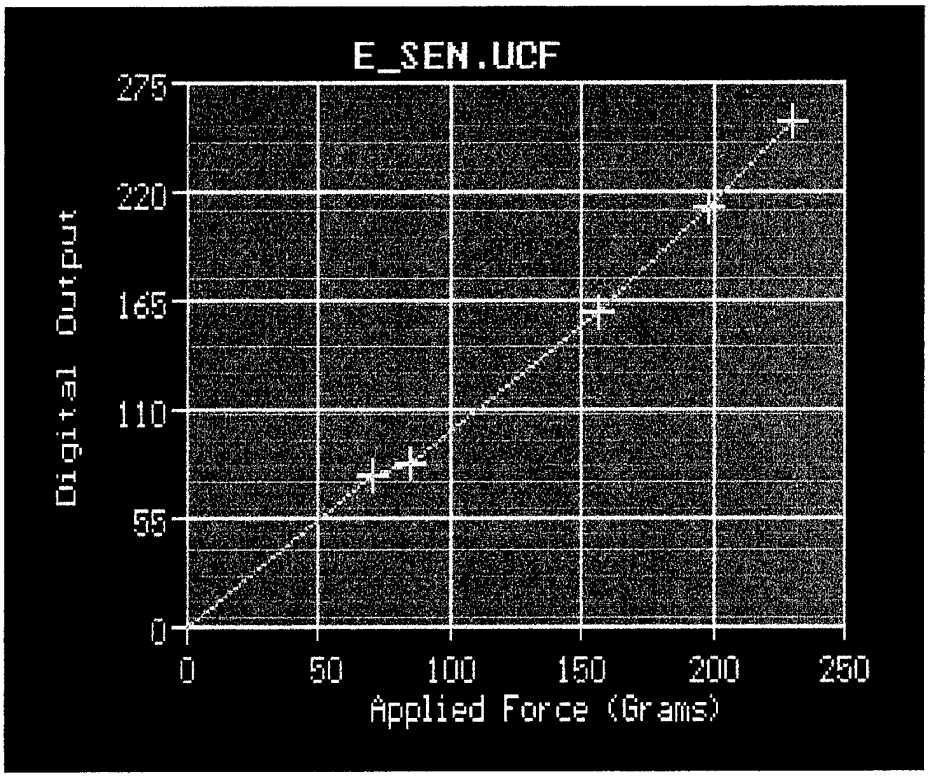

FIGURE 4 (a) Photo of force sensors, (b) Sensor calibration curve

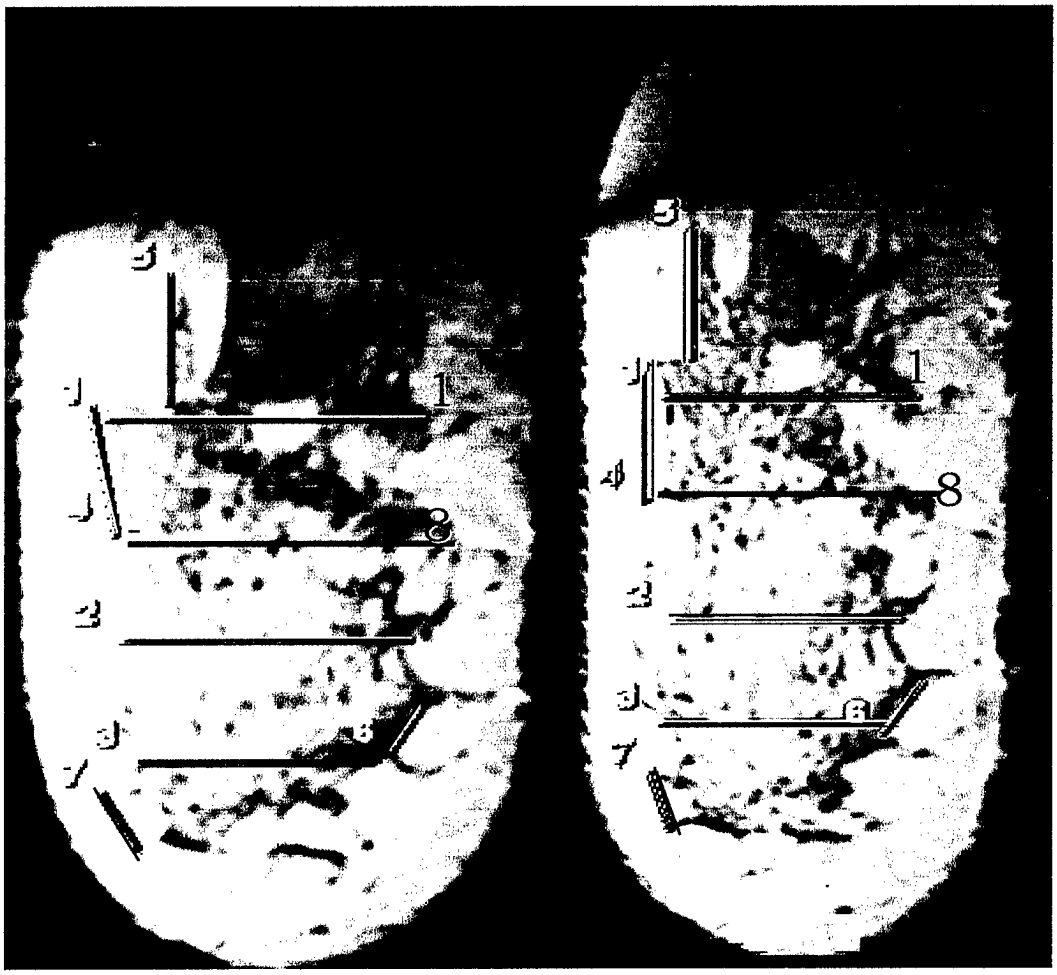

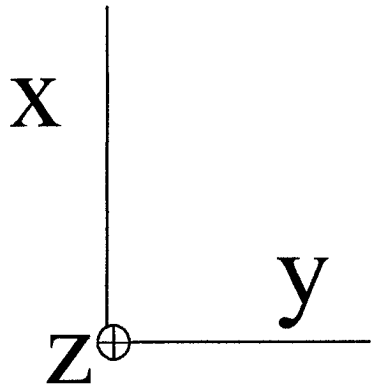

FIGURE 5. Images of line segments between paired points

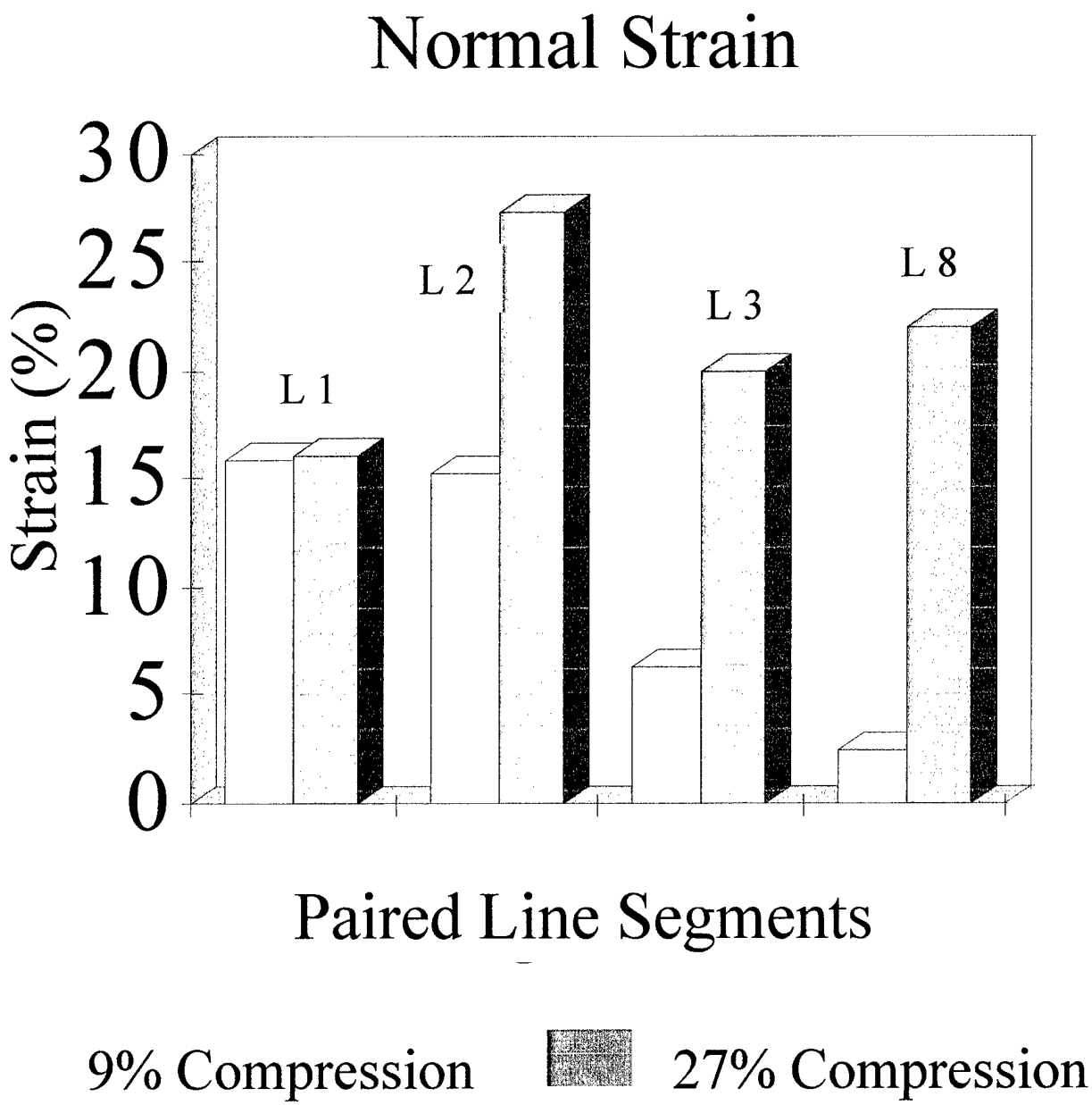

FIGURE 6. Graph of normal stress

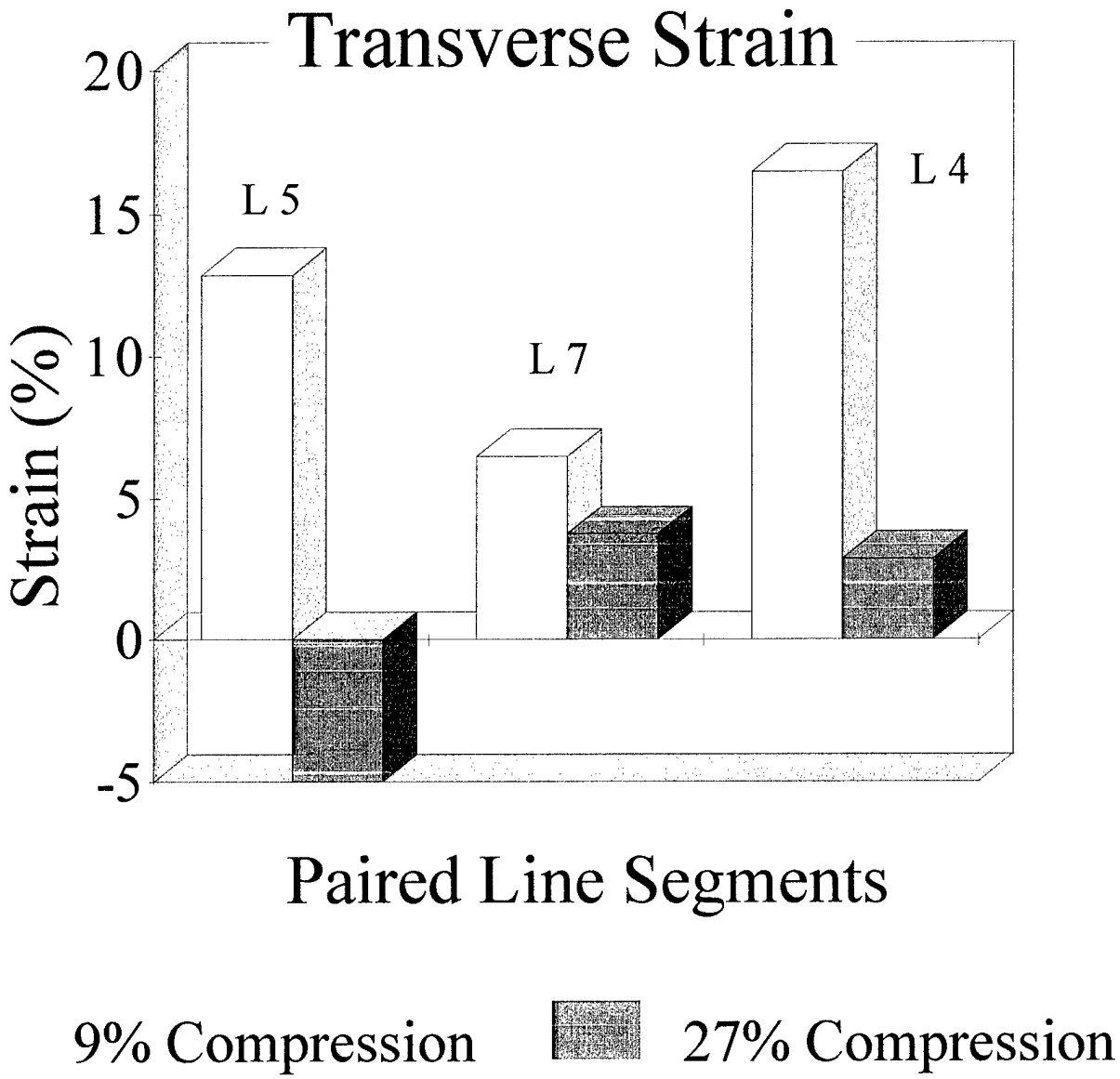

FIGURE 7. Graph of transverse stress

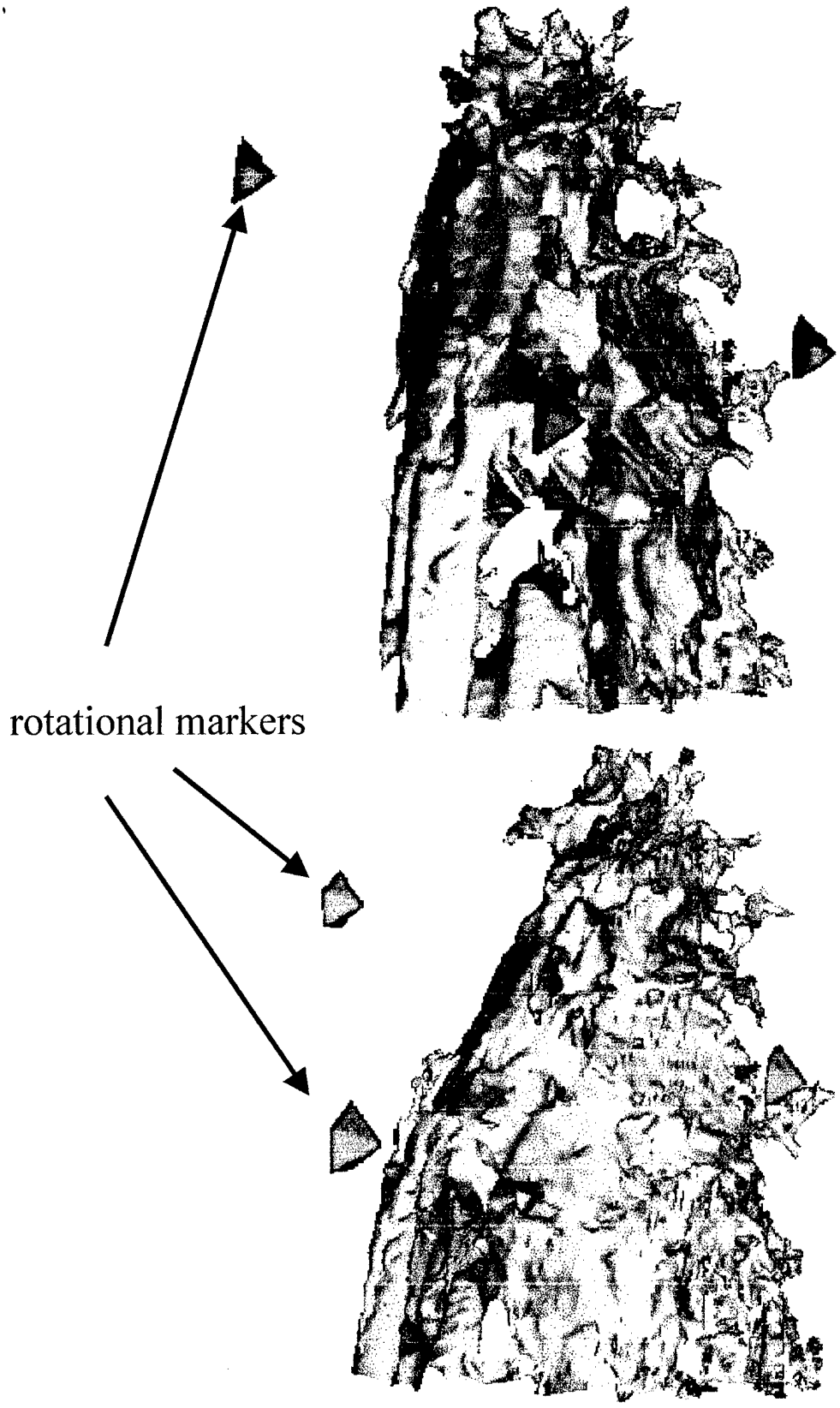

FIGURE 8. Volume of segmented data

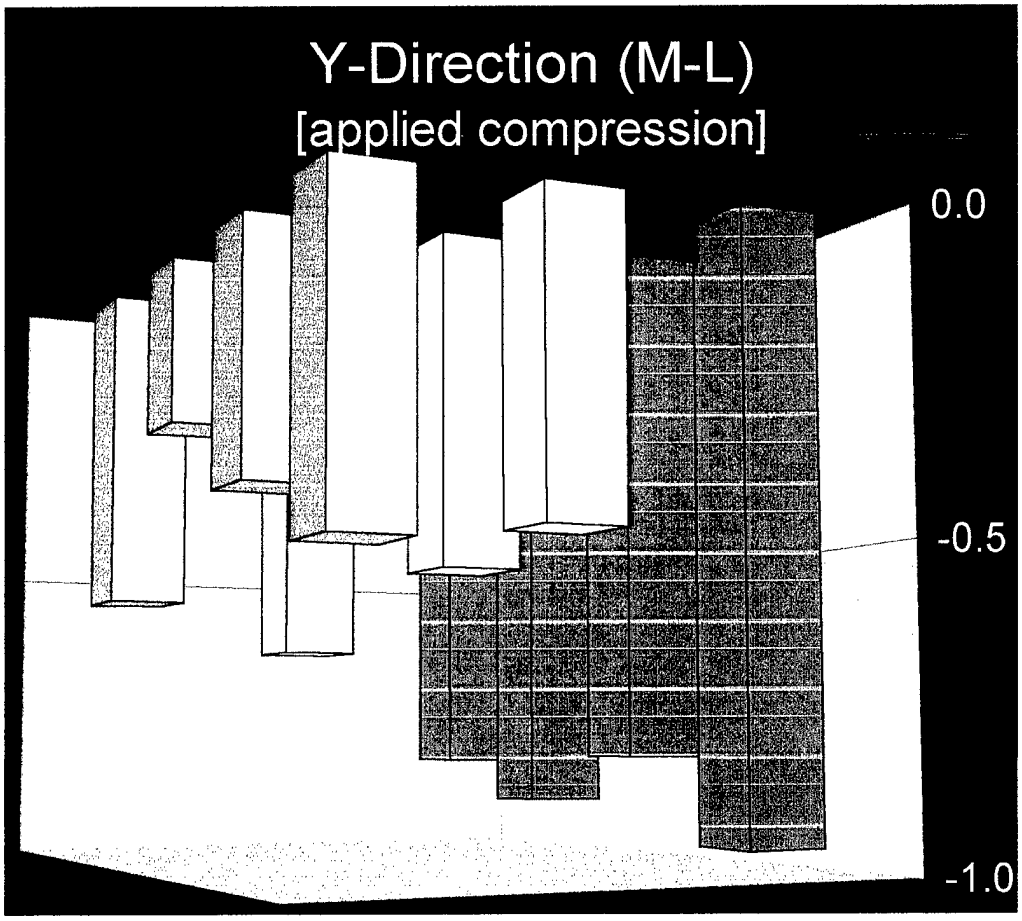

5 % compression

10% compression

15% compression

FIGURE 9 (a) Component of displacement vector in the direction of compression (medial/lateral)

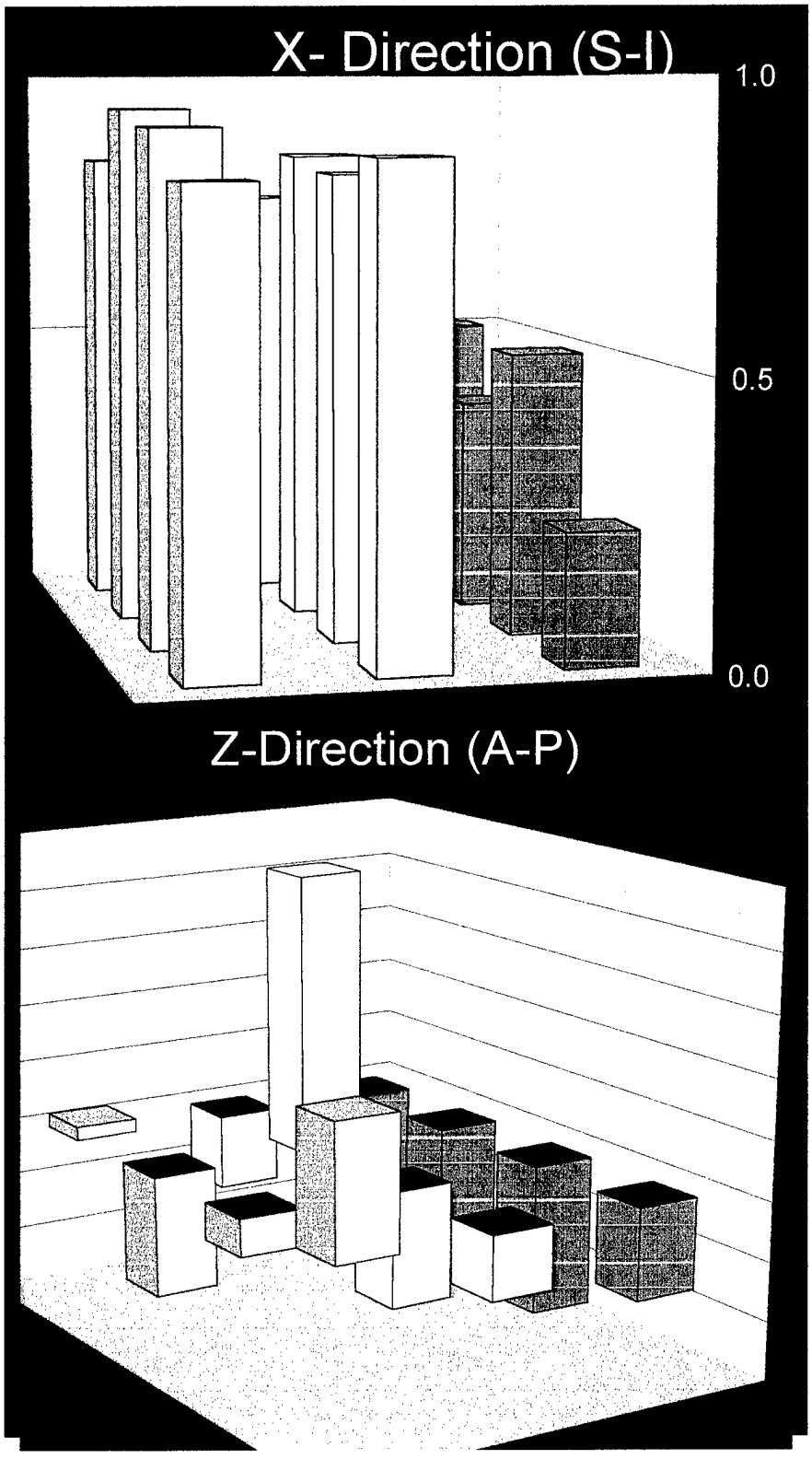

FIGURE 9. Components of displacement vector (b) transverse (S/I) and (c) out-of-plane (A/P)

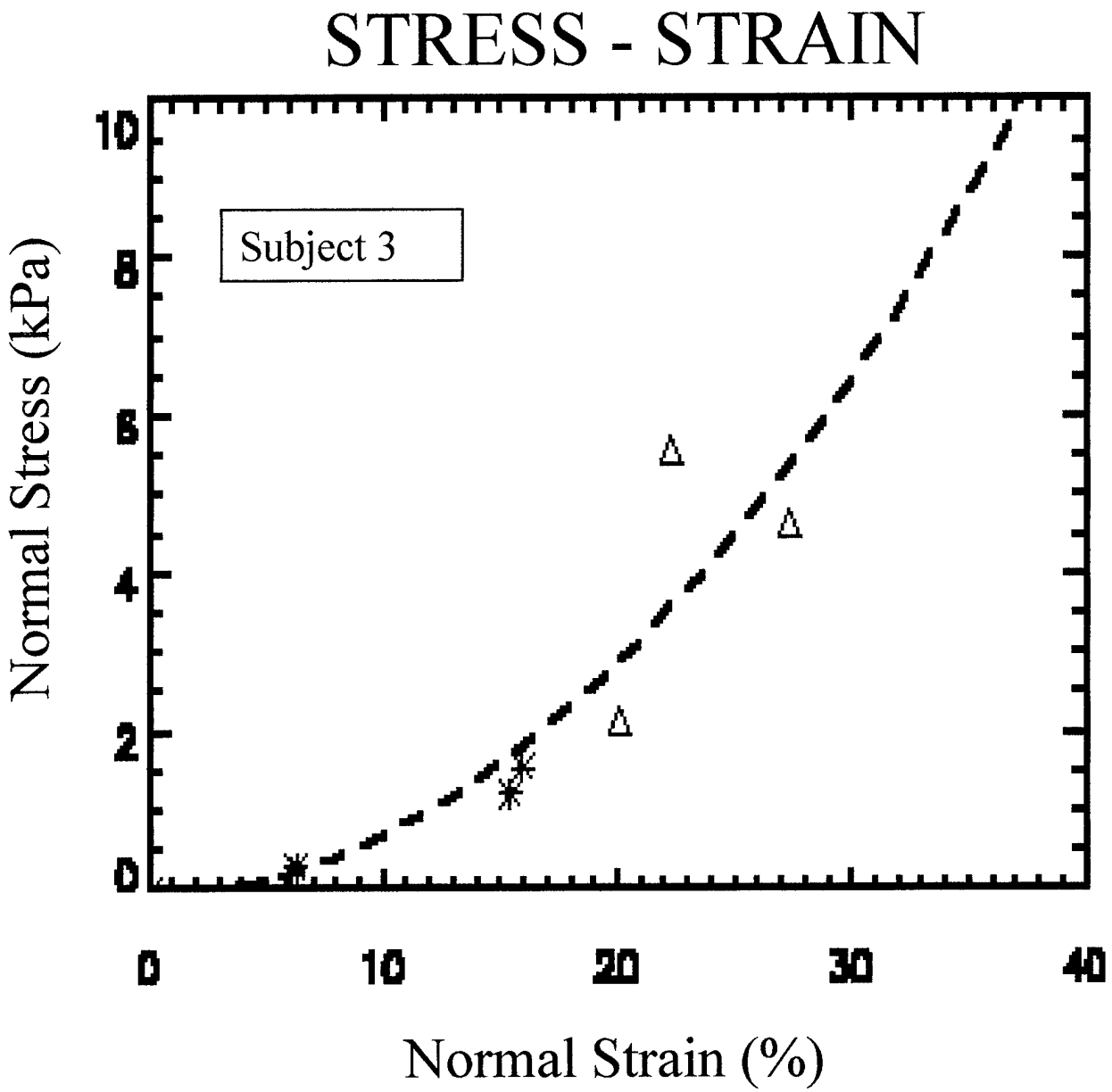

FIGURE 10 (a). Stress-strain curve of breast tissue

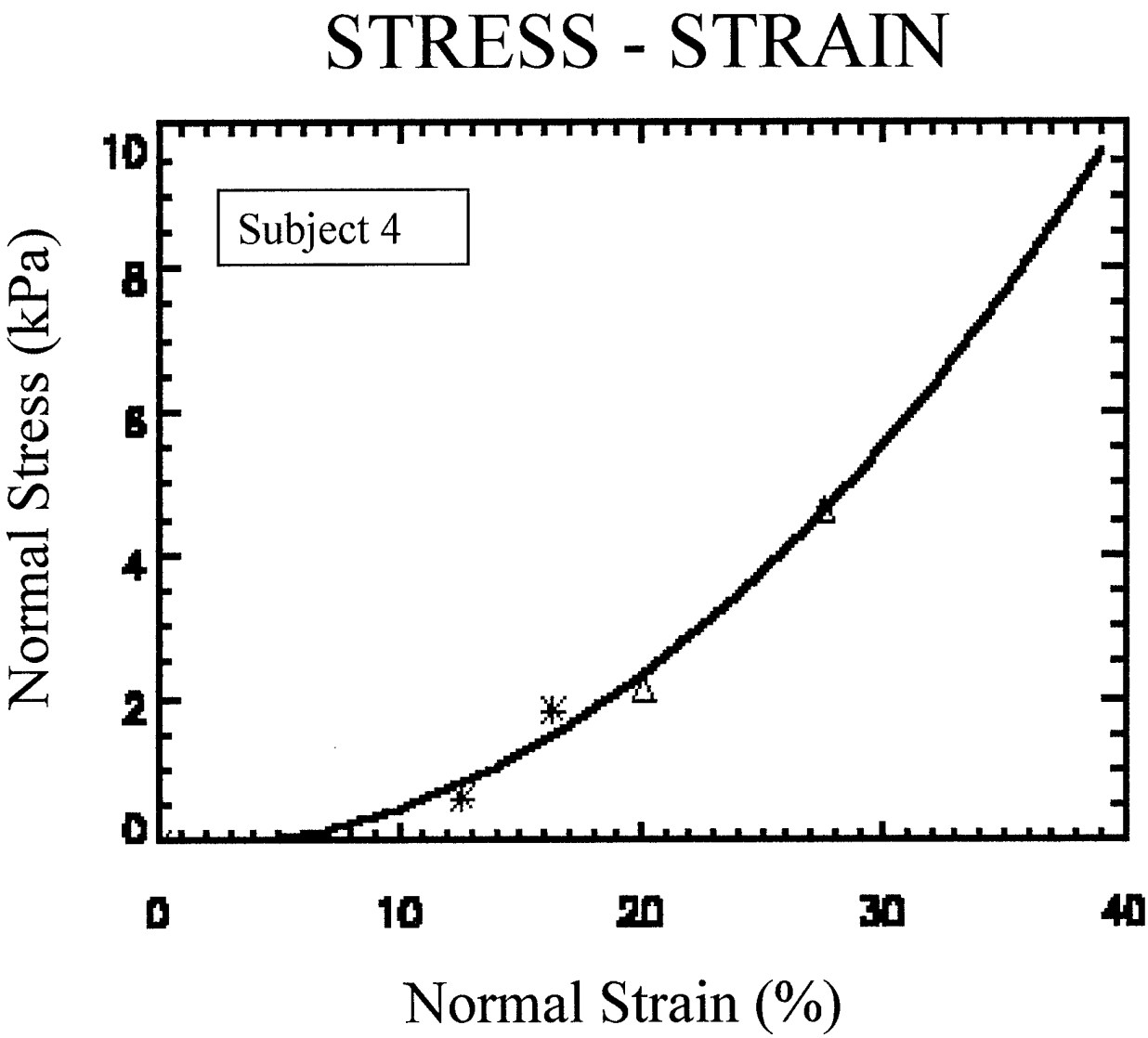

FIGURE 10 (b). Stress-strain curve of breast tissue

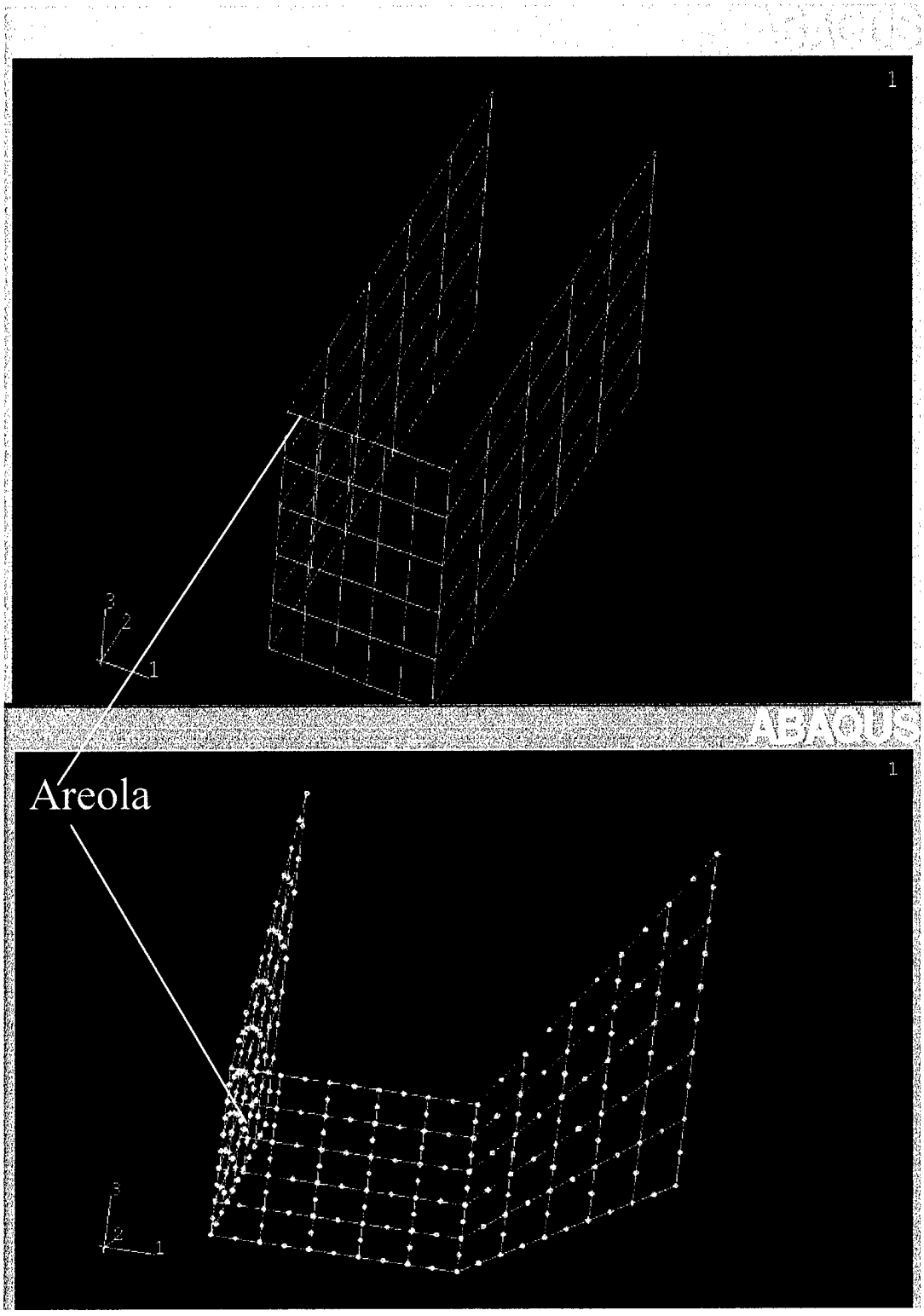

FIGURE 11 Simplified FEM nodal mesh coronal view of skin

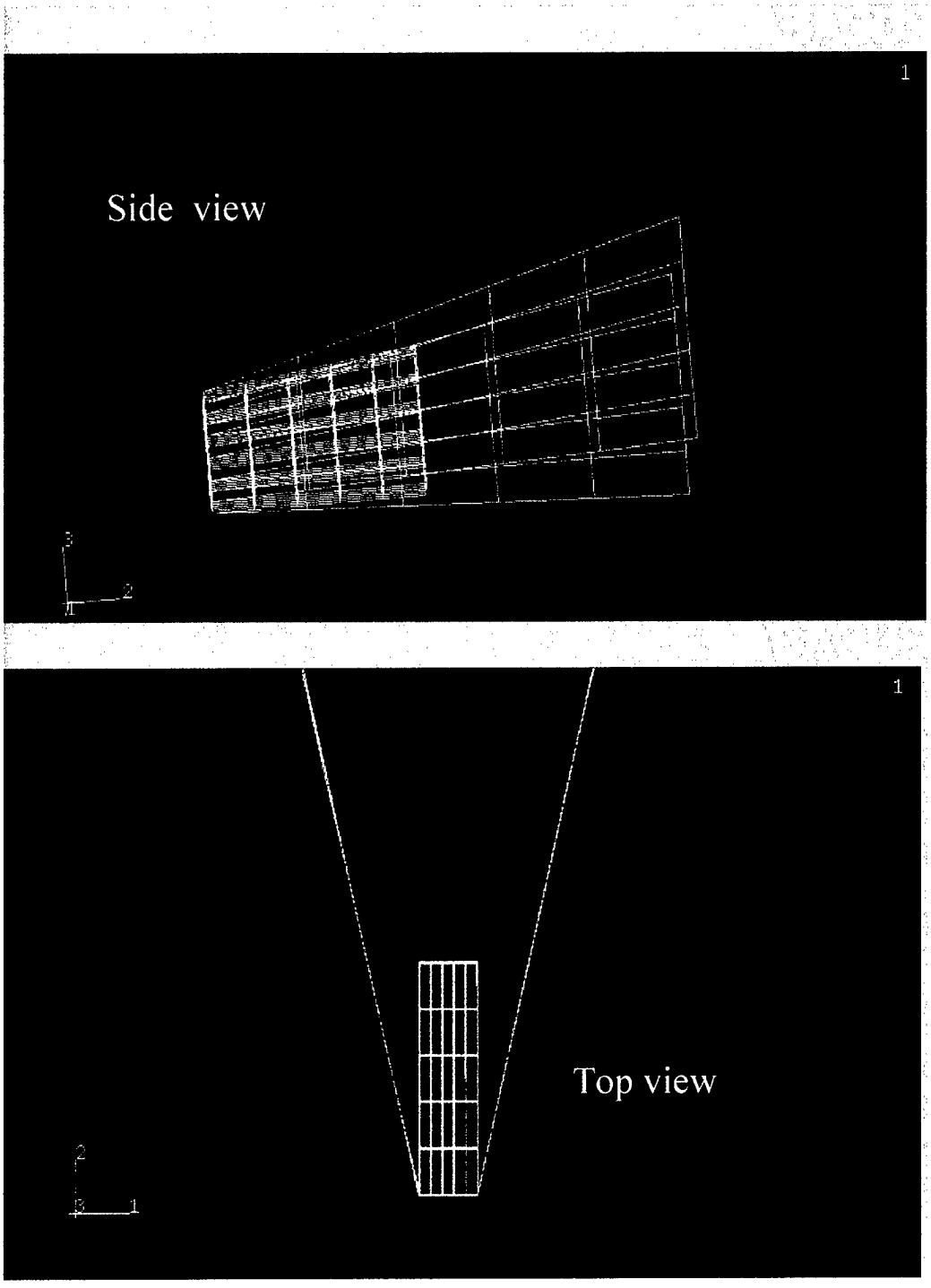

FIGURE 12. Nodal mesh of skin and tissue

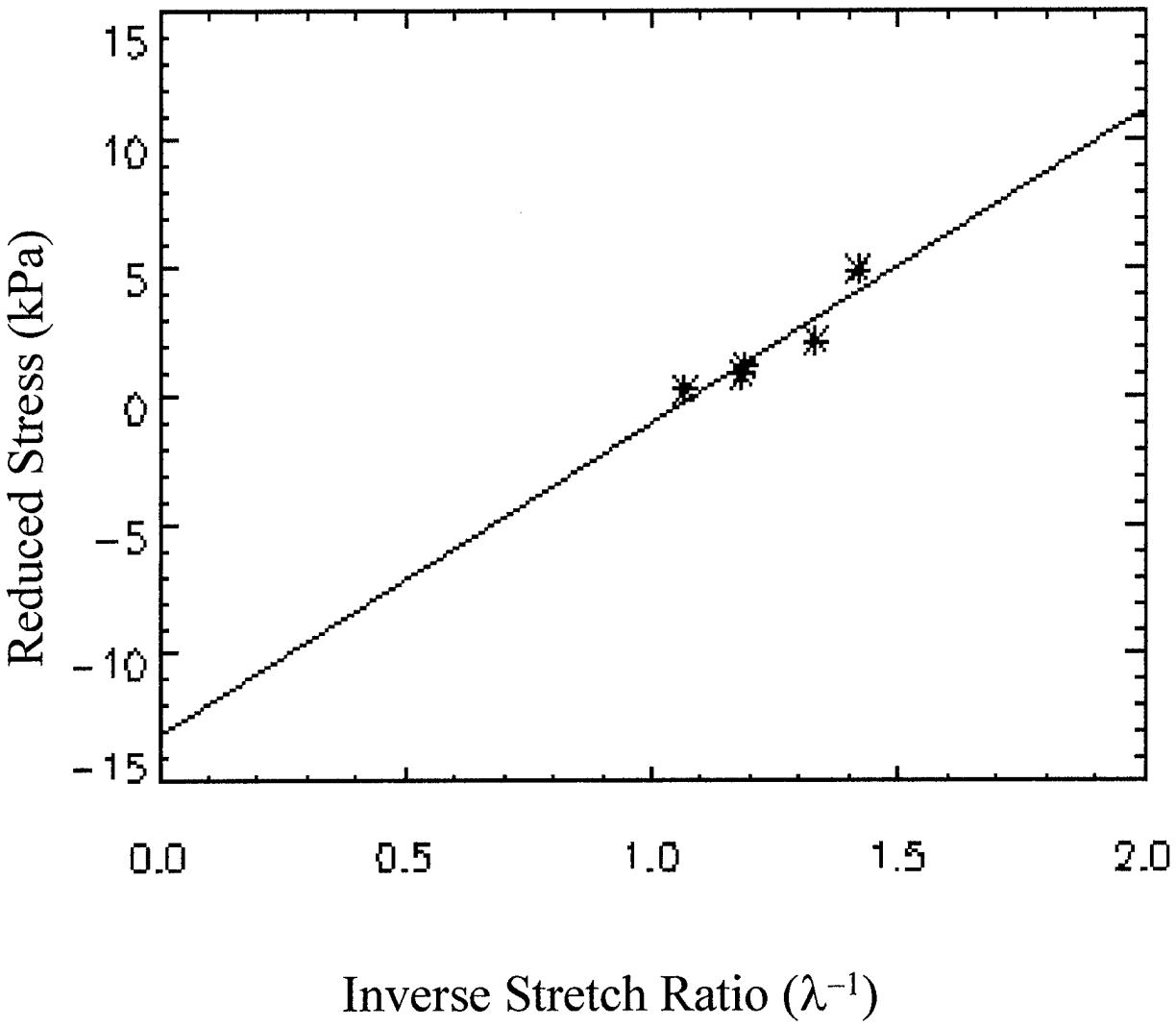

FIGURE 13. Reduced stress versus λ^{-1} curve using uniaxial experimental data

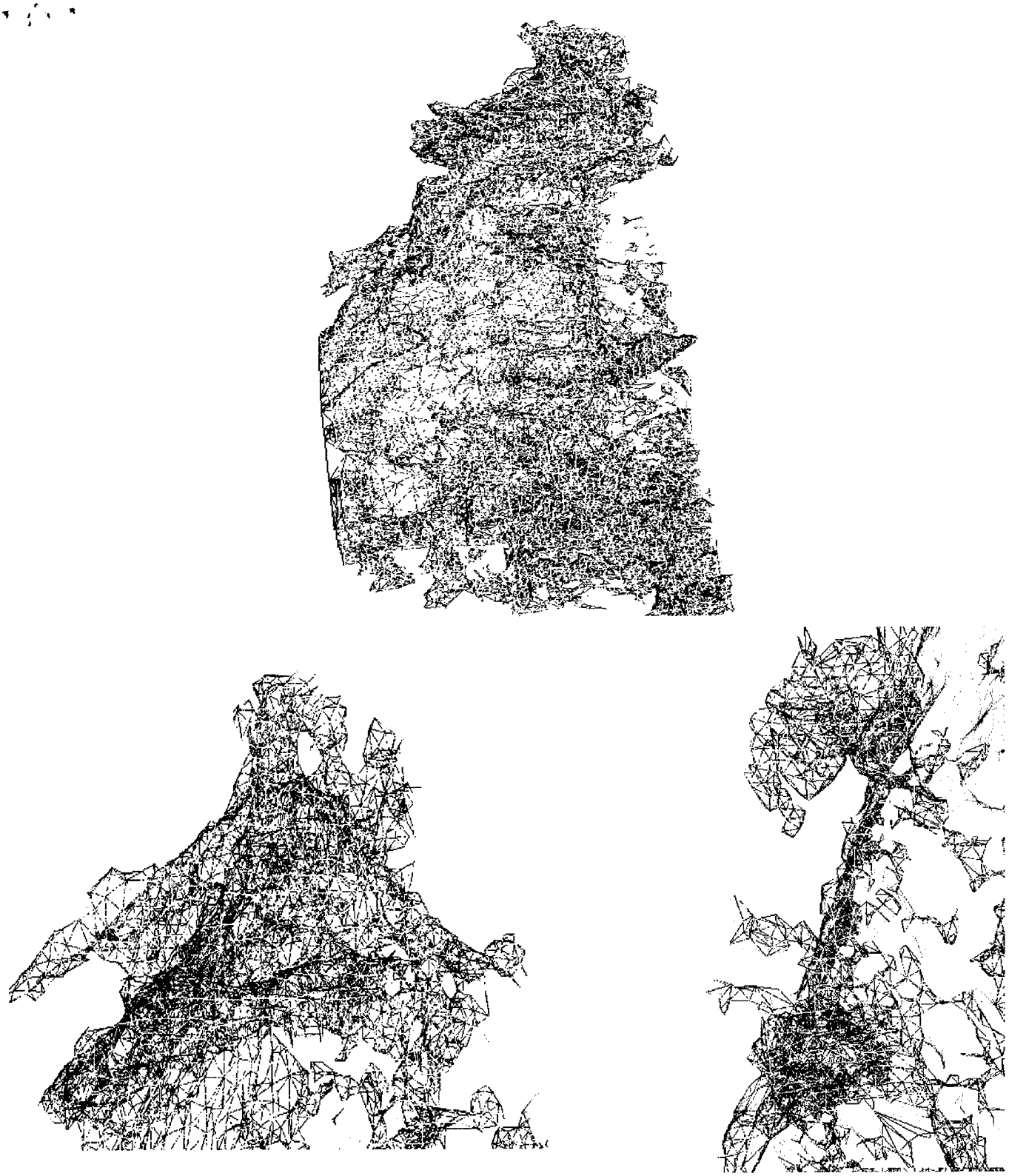

FIGURE 14. Complex mesh of segmented tissue using tetrahedral elements